Proc. 10th Int. Workshop on Neutrino-Nucleus Interactions in Few-GeV Region (NuInt15)
JPS Conf. Proc. **12**, 010018 (2016)
https://doi.org/10.7566/JPSCP.12.010018

CRPA Calculations for Neutrino-Nucleus Scattering : From Very Low Energies to the Quasielastic Peak

Natalie Jachowicz[1], Vishvas Pandey[1], Marco Martini[1,2], Raúl González-Jiménez[1], Tom Van Cuyck[1], Nils Van Dessel[1]

[1] *Department of Physics and Astronomy, Ghent University, Proeftuinstraat 86, B-9000 Gent, Belgium*
[2]*ESNT, CEA-Saclay, DSM, IRFU, Service de Physicque Nucléaire, F-91191 Gif-sur-Yvette Cedex, France*

E-mail: natalie.jachowicz@ugent.be

(Received January 31, 2016)

We present continuum random phase approximation calculations (CRPA) for neutrino-induced quasielastic scattering off atomic nuclei. The validity of our formalism is checked by a careful confrontation of its results with semi-inclusive double-differential electron scattering data. We pay special attention to excitations in the giant resonance region. The CRPA is well-suited for the description of interactions in this energy range. We aim at providing a uniform description of one-nucleon knockout processes over the whole energy range from threshold to the quasielastic peak. Our calculations point to the fact that low-energy and giant-resonance excitations provide a non-negligible contribution to the interaction strength, especially at forward lepton-scattering angles.

KEYWORDS: neutrino-nucleus interactions, quasielastic scattering

1. Introduction

Quasielastic scattering is an important reaction mechanism in accelerator-based neutrino-oscillation experiments. As neutrinos are produced with a wide range of energies, an accurate description of the reaction process over this whole energy range is important. A continuum random phase approximation approach that was designed for the description of neutrino-scattering reactions in the giant resonance region [1, 2] was extended and adapted for the calculations of cross sections in the quasielastic-peak regime [3, 4]. In this way, we obtain a consistent treatment of cross sections over the whole energy range relevant for quasielastic scattering processes.

2. Mean field model

A key element in the model presented here is the non-relativistic impulse approximation. The Hartree-Fock (HF) single-particle bound-states and the continuum wave functions are obtained by solving the Schrödinger equation using an effective Skyrme interaction. The SkE2 Skyrme parameterization's optimization is based on a fit to ground-state and low-lying excited state properties of spherical nuclei [5, 6]. The fact that the outgoing nucleon's wave function is generated in a (real) nuclear potential partially includes final-state interactions, in a natural way. The influence of the spreading width of the particle states is taken into account using a folding procedure [4]. For charged-current interactions, at low energies of the outgoing lepton the impact of the Coulomb potential of the nucleus on the outgoing lepton can be taken into account using a Fermi function. At intermediate energies, Coulomb corrections for the outgoing lepton are implemented using a modified effective momentum approach (MEMA) [7]. As the description of the nuclear dynamics is non-relativistic, relativistic corrections are implemented based on the effective scheme proposed in Ref. [8]. In this work, dipole form factors and an axial mass $M_A = 1.03$ GeV are used.

3. Long-range correlations

Long-range correlations are introduced using a continuum random phase approximation approach. The CRPA is based on a Green's function formalism, where the CRPA propagator is obtained by the iteration to all orders of the first-order contribution to the particle-hole Green's function

$$\Pi_{RPA}(x_1, x_2; E_x) = \Pi_0(x_1, x_2; E_x) + \frac{1}{\hbar}\int dx dx' \Pi_0(x_1, x; E_x)\tilde{V}(x, x')\Pi_{RPA}(x', x_2; E_x), \quad (1)$$

with $\tilde{V}$ the antisymmetrized Skyrme residual interaction.

The same Skyrme SkE2 parameterization that is used to generate the Hartree-Fock single-particle wave functions is used as *ph*-interaction in the RPA calculation, assuring consistency of the formalism with regards to the nucleon interaction. The Q^2 running of the residual interaction is controled by a dipole form-factor at the nucleon vertices [4].

The CRPA wave-functions and transition densities are then related to the unperturbed ones through :

$$\begin{aligned}\left|\Psi_C^{RPA}(E)\right\rangle &= \left|ph^{-1}(E)\right\rangle + \int dx_1 \int dx_2 \ \widetilde{V}(x_1, x_2) \\ &\sum_{c'} \mathcal{P} \int d\varepsilon_{p'} \left[\frac{\psi_{h'}(x_1)\psi^{\dagger}_{p'}(x_1, \varepsilon_{p'})}{E - \varepsilon_{p'h'}} \left|p'h'^{-1}(\varepsilon_{p'h'})\right\rangle \right. \\ &\left. - \frac{\psi^{\dagger}_{h'}(x_1)\psi_{p'}(x_1, \varepsilon_{p'})}{E + \varepsilon_{p'h'}} \left|h'p'^{-1}(-\varepsilon_{p'h'})\right\rangle \right] \left\langle \Psi_0 \left| \hat{\psi}^{\dagger}(x_2)\hat{\psi}(x_2) \right| \Psi_C(E) \right\rangle .\end{aligned} \quad (2)$$

These wave functions are of the standard RPA-form

$$|\Psi^C_{RPA}\rangle = \sum_{C'} \left[X_{C,C'}|p'h'^{-1}\rangle - Y_{C,C'}|h'h'^{-1}\rangle \right], \quad (3)$$

with

$$\begin{aligned}X_{C,C'}(E, \varepsilon_{p'}) &= \delta_{C,C'} \ \delta(E - \varepsilon_{p'h'}) + \ \mathcal{P} \int dx_1 \int dx_2 \ \widetilde{V}(x_1, x_2) \\ &\qquad \frac{\psi_{h'}(x_1)\psi^{\dagger}_{p'}(x_1, \varepsilon_{p'})}{E - \varepsilon_{p'h'}} \left\langle \Psi_0 \left| \hat{\psi}^{\dagger}(x_2)\hat{\psi}(x_2) \right| \Psi_C(E) \right\rangle\end{aligned} \quad (4)$$

and

$$\begin{aligned}Y_{C,C'}(E, \varepsilon_{p'}) &= \int dx_1 \int dx_2 \ \widetilde{V}(x_1, x_2) \\ &\qquad \frac{\psi^{\dagger}_{h'}(x_1)\psi_{p'}(x_1, \varepsilon_{p'})}{E + \varepsilon_{p'h'}} \left\langle \Psi_0 \left| \hat{\psi}^{\dagger}(x_2)\hat{\psi}(x_2) \right| \Psi_C(E) \right\rangle .\end{aligned} \quad (5)$$

C denotes all quantum numbers representing an accessible channel. These equations reflect the fact that RPA wave functions are a superposition of ph- and hp-excitations, out of a correlated ground state.

4. Quasielastic electron scattering

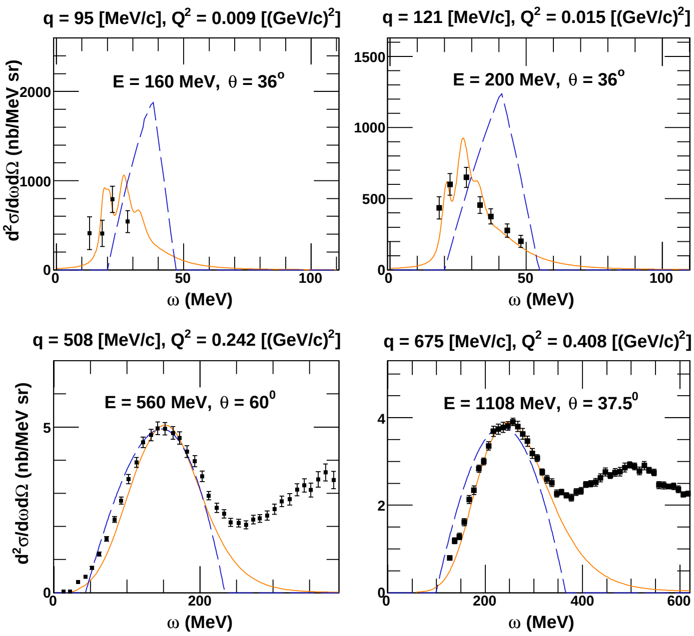

Fig. 1. Comparison between Fermi gas (FG) [10] (dashed) and HF-CRPA (solid) cross sections for electron scattering off ^{12}C. Data was taken from Refs. [11, 12]

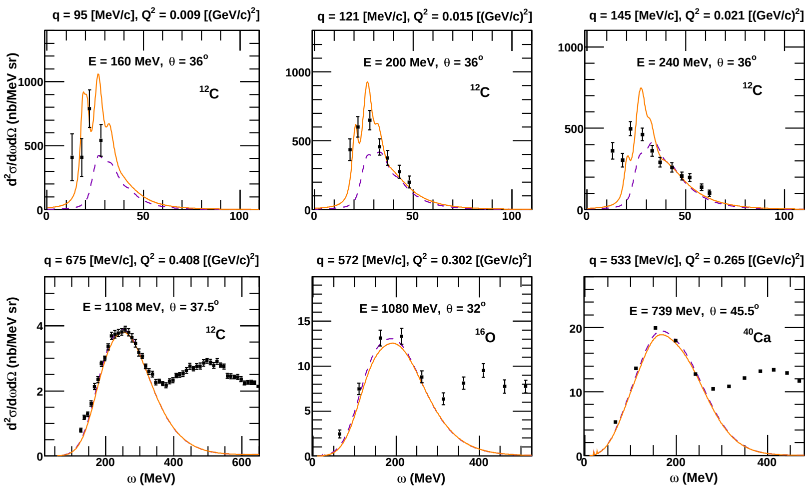

Fig. 2. Comparison between CRPA cross section calculations and electron scattering data. The full line represents CRPA cross sections, the dashed line Hartree-Fock calculations. Data was taken from Refs. [11–14].

The strength of the formalism presented here lies in its ability to describe low-energy excitations as well as excitations in the quasielastic regime. Whereas Fermi gas calculations are well-known to provide an effective and efficient tool for the description of cross section in the quasielastic peak region, Fig. 1 shows that Fermi gas calculations tend to fall short when confronted with leptons with energies below a few hundreds of MeV. For incoming energies around 200 MeV and lower, the responses are dominated by low-energy effects that are inaccessible in a Fermi-gas approach.

Figure 2 shows a comparison between our cross section calculations and double-differential semi-inclusive electron scattering data for three different target nuclei over a broad range of four-momentum transfer. The overall agreement between our model and the data is very satisfactory.

5. CC Quasielastic ν_μ scattering off ^{12}C

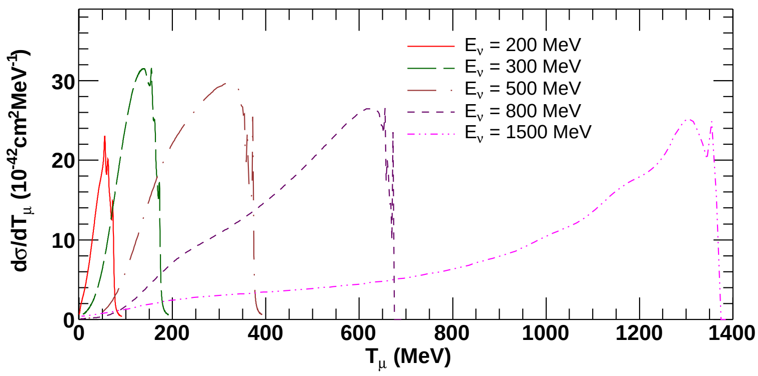

Fig. 3. Differential cross sections for the process $^{12}\mathrm{C}(\nu_\mu, \mu^-)^{12}\mathrm{N}^*$ for a range of incoming neutrino energies.

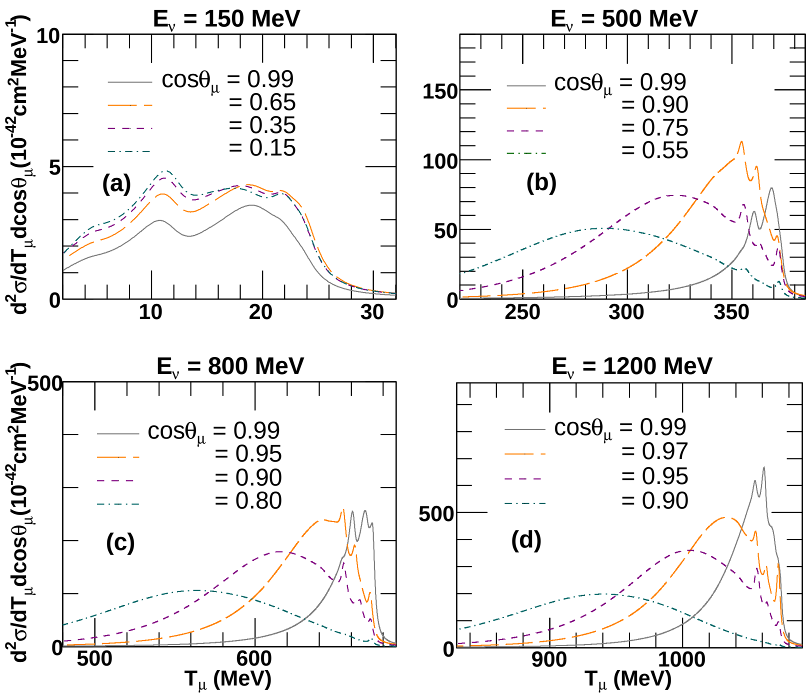

Fig. 4. Double differential cross sections for forward scattering in CC muon neutrino scattering off ^{12}C

This agreement lends confidence to the validity of the formalism in the prediction of neutrino-scattering cross sections. In Figure 3 we show our cross-section predictions for cross sections with incoming energies ranging between 200 MeV and 1500 MeV. It is evident from the figure that with increasing incoming neutrino energies, the strength of the cross sections shifts to higher muon energies. There is moreover a clear signature of the low-ω excitations, even at neutrino energies around and beyond the peak of the MiniBooNE [15] and T2K [16] muon-neutrino energy-distributions.

In Fig. 4, we show double differential cross section for different values of the outgoing lepton's direction. For incoming neutrino energy E_ν= 150 MeV, the double differential cross section is dominated by low-lying nuclear excitations. For neutrino energies around the average energy of the MiniBooNE [15] and T2K [16] fluxes, the contributions from nuclear collective excitations are still sizable for forward muon scattering angles. The same feature is even still visible for very forward scattering of neutrinos with an energy of 1200 MeV. The contribution of collective excitations to neutrino-nucleus responses cannot be accounted for within relativistic FG-based simulation codes. As evident from the results presented here, they can account for non-negligible contributions to the signal.

6. Electron neutrinos

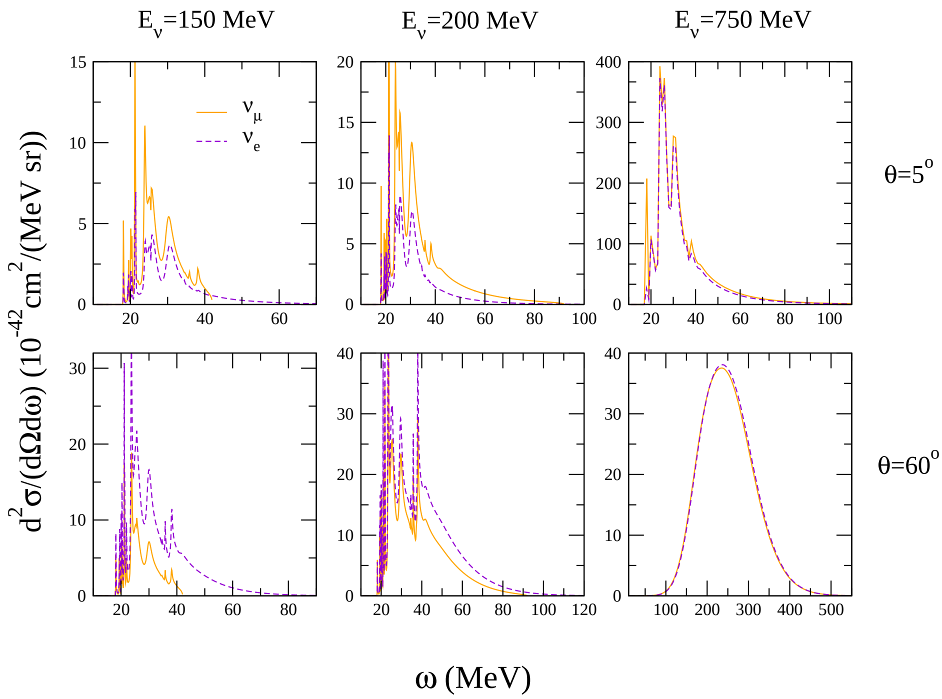

Fig. 5. Comparison between double differential electron neutrino and muon neutrino-induced cross sections off ^{12}C as a function of the energy transfer to the nucleus for fixed values of the incoming neutrino energy.

The lion's share of cross section data that were published in recent years focus on charged-current muon-neutrino scattering. Recently however, double-differential inclusive ν_e CC scattering cross sections were reported by the T2K and MINERνA collaborations [17, 18].

As the differences between muon neutrino and electron neutrino-induced cross sections are due to the different mass of the outgoing charged lepton in both processes, these differences can be expected to be most pronounced for low-energy reactions. Hence we present an analysis [19] of these

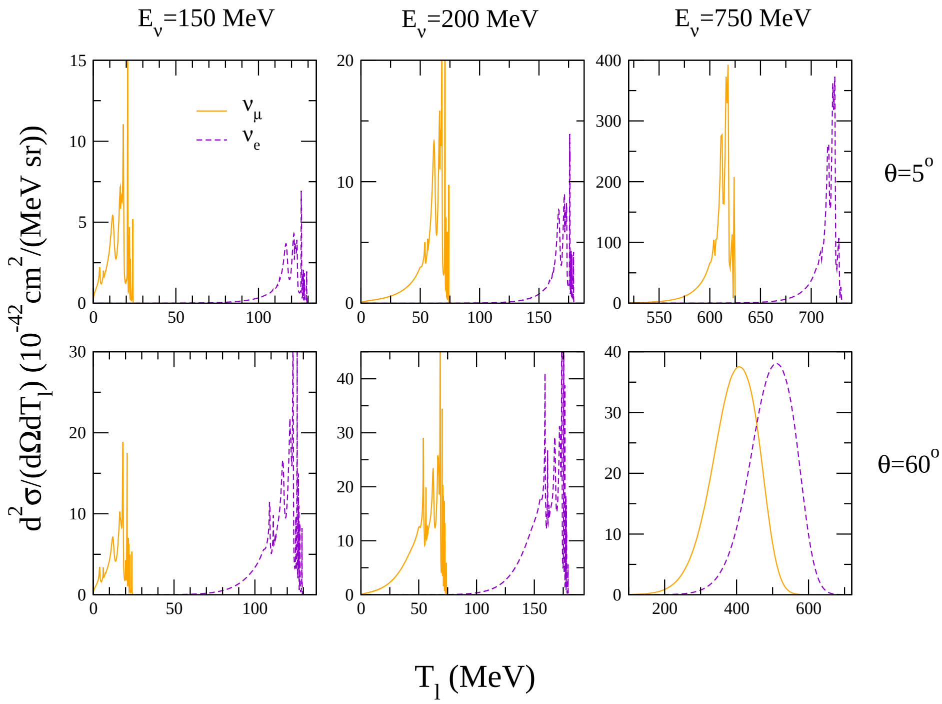

Fig. 6. Comparison between double differential electron neutrino and muon neutrino-induced cross sections off ^{12}C as a function of the kinetic energy of the final lepton, for fixed values of the incoming neutrino energy.

differences within the framework developed in the previous sections.

Figure 5 shows electron neutrino and muon neutrino-induced processes as a function of the energy transfer to the nucleus. As expected, the differences between these processes are small for reactions at relatively high energy. For smaller incoming energies and forward scattering however, the differences are considerable and in some cases quite surprising. It is remarkable that for low energy processes and forward scattering angles muon neutrino-induced processes dominate the electron neutrino ones. This is related to the fact that cross sections not only depend on nuclear response functions but also on lepton kinematics. Reactions at low energies and for forward lepton scattering angles are dominated by Coulomb and longitudinal contributions to the cross section. The relative weight of CL and T contributions is the result of a subtle interplay between lepton kinematic factors and response functions. The competition for dominance of the cross section between both, is very sensitive to energy and momentum transfer. The surprising dominance of ν_μ over ν_e cross sections is related to this and dictated by the non-trivial dependence of momentum transfer on lepton mass and scattering angle for forward scattering.

It should be kept in mind that even when nuclear responses are comparable, the energy of the reaction products i.e. the signal in the detector, can differ considerably [19]. This is illustrated in Fig. 6, where cross sections are shown for the same processes as illustrated in Fig. 5, but now as a function of the kinetic energy of the outgoing lepton. Apart from the obvious differences in energy threshold, the figures illustrate the shift to lower kinetic energies for muon neutrino compared to electron neutrino-induced processes. At low incoming energies and forward lepton scattering angles this also results in a higher cross section for processes with a muon in the final state.

Summarizing, we presented a description of quasielastic neutrino-induced scattering off atomic nuclei, that is able to describe nucleon-knockout processes for a range of energy transfers starting from threshold up to the quasielastic peak regime. Our results suggest that for forward lepton scattering, low-energy excitations provide some extra strength to the quasielastic response in accelerator-based experiments. At low energies, some non-trivial differences between electron neutrino and muon neutrino-induced cross section arise.

Acknowledgments. This work was supported by the Interuniversity Attraction Poles Programme P7/12 initiated by the Belgian Science Policy Office and the Research Foundation Flanders (FWO-Flanders). The computational resources (Stevin Supercomputer Infrastructure) and services used in this work were provided by Ghent University, the Hercules Foundation and the Flemish Government.

References

[1] N. Jachowicz, S. Rombouts, K. Heyde, and J. Ryckebusch, Phys. Rev. C**59** (1999) 3246.
[2] N. Jachowicz, K. Heyde, J. Ryckebusch, and S. Rombouts, Phys. Rev. C**65** (2001) 025501.
[3] V. Pandey, N. Jachowicz, J. Ryckebusch, T. Van Cuyck, and W. Cosyn, Phys. Rev. C**89** (2014) 024601.
[4] V. Pandey, N. Jachowicz, T. Van Cuyck, J. Ryckebusch, and M. Martini, Phys. Rev. C**92** (2015) 024606.
[5] J. Ryckebusch, M. Waroquier, K. Heyde, J. Moreau, and D. Ryckbosch, Nucl. Phys. A**476** (1988) 237.
[6] J. Ryckebusch, K. Heyde, D. Van Neck, and M. Waroquier, Nucl. Phys. A**503**, (1989) 694.
[7] J. Engel, Phys. Rev. C**57** (1998) 2004.
[8] S. Jeschonnek, T. W. Donnelly, Phys. Rev. C**57** (1998) 2438
[9] N. Jachowicz, K. Vantournhout, J. Ryckebusch, and K. Heyde, Phys. Rev. Lett. **93** (2004) 082501
[10] J.E. Amaro, M.B. Barbaro, J.A. Caballero, T.W. Donnelly, and C. Maieron Phys. Rev. C**71** (2005) 065501.
[11] P. Barreau et al., Nucl. Phys. A**402** (1983) 515.
[12] R. M. Sealock et al., Phys. Rev. Lett. **62** (1989) 1350.
[13] M. Anghinolfi et al., Nucl. Phys. A**602** (1996) 405.
[14] C. F. Williamsonet al., Phys. Rev. C**56** (1997) 3152.
[15] A. A. Aguilar-Arevalo et al., (MiniBooNE Collaboration), Phys. Rev. D**81**, (2010) 092005.
[16] K. Abe et al., (T2K Collaboration), Phys. Rev. D**87** (2013) 092003.
[17] K. Abe et al., (T2K Collaboration), Phys. Rev. Lett.**113** (2014) 241803.
[18] J. Wolcott et al. (MINERνA Collaboration), arXiv:1509.05729 [hep-ex].
[19] M. Martini, N. Jachowicz, M. Ericson, V. Pandey, T. Van Cuyck, N. Van Dessel, submitted to Phys. Rev. C.